

Computational fluid dynamic simulation of a gas-solid fluidized bed system: A dense phase analysis



L.P. Olivo-Arias¹, L.G. De Araujo², J.B. Rojas-Trigos¹

¹Instituto Politécnico Nacional, Centro de Investigación en Ciencia Aplicada y Tecnología Avanzada Unidad Legaria. Legaria No. 694 Colonia Irrigación, C.P. 11500 Ciudad de México, México.

²Nuclear and Energy Research Institute, IPEN-CNEN/SP. Av. Prof. Lineu Prestes, 2242-Butantã, São Paulo, SP CEP 05508-000, Brazil.

E-mail: lolivoa1500@alumno.ipn.mx

(Received 20 November 2019, accepted 30 December 2019)

Resumen

El estudio del sistema gas-sólido fue realizado a través de un análisis de dinámica computacional de fluidos (DCF) en un reactor de lecho fluidizado. Este proceso inicia con la interacción entre las partículas y la fase gaseosa. El análisis del proceso de fluidización se logra a través de una aproximación Euleriana representada en el comportamiento de la dinámica de la fase sólida durante el proceso de expansión del lecho. Dentro del proceso se demostró la formación de la fase densa y cómo podría afectar, los efectos de la temperatura, la presión y la velocidad superficial del gas en el sistema de lecho fluidizado. El propósito de este trabajo es establecer parámetros hidrodinámicos evaluando la fracción volumétrica de las partículas y el perfil de velocidad axial y radial empleando los modelos de arrastre de Syamlal O'Brien y Gibilaro. Además, que se debe tener en cuenta en un análisis de dinámica computacional de fluidos, como la generación de la malla, la selección de los modelos, y el tiempo de corrida de la simulación. Los resultados de las simulaciones mostraron que la concentración de la fase sólida ha tenido una distribución uniforme, una formación de la fase densa, dado a los cambios de condiciones de operación y una razonable expansión del lecho en el tiempo final de simulación.

Palabras claves: Dinámica de Fluidos Computacional, Reactor de Lecho Fluidizado, Sistema de Dos fases, Modelo Hidrodinámico, Fracción Volumétrica del Sólido y Fase Densa.

Abstract

The study of the gas-solid system was performed through an analysis of computational fluid dynamics (CFD) in a fluidized bed reactor. This process begins with the interaction between the particles and the gas phase. The fluidization process analysis is achieved through the Eulerian approach represented in the behavior of the solid phase dynamics during the bed expansion process. Within the process, the formation of the dense phase was demonstrated and how it could affect the effects of temperature, pressure and surface velocity of the gas in the fluidized bed system. The purpose of this work is to establish hydrodynamic parameters by evaluating the volumetric fraction of the particles and the axial and radial velocity profile using the drag models of Syamlal O'Brien and Gibilaro. In addition, it should be considered the analysis of the computational dynamics of fluids, such as the generation of the mesh, the selection of the models, and the run time of the simulation. The results of the simulations showed that the solid phase concentration has had a uniform distribution, a dense phase formation, given the changes in operating conditions and a reasonable expansion of the bed in the final simulation time.

Keywords: Computational Fluid Dynamic, Fluidized Bed reactor, Two-Phase system, Hydrodynamic model, Solid volume fraction, Dense phase.

PACS: 47.11.-j, 82.60.-s, 47.55. Lm, 47.85. Dh

ISSN 1870-9095

I. INTRODUCTION

Gas-solid fluidized bed reactors are found in a wide range of industrial applications, such as petrochemical, water treatment and biotechnology processes, among others. However, more works have focused on the dynamic behavior of the two-phase flow structures in actual fluidized processes so that they are well understood and effectively quantified due to the complexity of the gas-solid interactions.

Many models with simple assumptions have been suggested to describe the behavior of the two phases. These models have been widely introduced by many researchers. They have explained and made sense of the main features of the hydrodynamic parameters in a fluidized bed and have been of great help in improving knowledge of the interaction between the two phases.

The simulation of the solid-gas system has been analyzed throughout the studies in fluidized bed reactors for different types of processes in the industry. In order to study the

hydrodynamics of the systems, interactions between the phases, and bed expansions, among other aspects related to the fluidization process, were calculated.

The importance of fluidized bed system hydrodynamic studies includes the interactions in the gas-solid system, the volume fractions, minimum fluidization velocity, and porosity among others. The purpose of those works is to improve the design conditions of the reactors and also the selection of materials that will be used in the fluid dynamics study.

The following are some works in the literature available that include the study of fluctuations of solids Kallio and Peltola [1], Kuramoto and Tanaka [2], Liang and Zhu [3], and Natarajan and Velraj [4]. They analyzed the variation of solids volume fractions in measurements and simulations of a bubbling fluidization reactor. The kinetic theory of granular flow (KTGF) is a tool developed from the kinetic theory of gases to describe the kinematics found in granular media, being one of the most utilized tools. It means an extension of the classical kinetic theory of gases to dense particulate flows.

These studies are supported by the research about the hydrodynamic of fluidized bed reactors incorporating the kinetic theory of granular flow (KTGF) Ding and Gidaspow [5], Zimmermann and Taghipour F. [6], Taghipour, F., Ellis, N., & Wong, C [7], PC Johnson [8], and Benzarti and Mhiri [9]. Also, there are many investigations for solid-liquid systems where different parameters are determined and some of them were used as the base for the present research.

Gidaspow *et al.* [10]. suggested an “effective restitution coefficient” near to unity. In the studies of Roy and Dudukovic [11] and Lettieri, P., Cammarata, L., Micale, G.D.M., Yates, J., [12], the granular flow model was applied to liquid-fluidized beds, with coefficients of restitution smaller than unity (implying inelastic collisions between particles) and with no explicit consideration of whether or not the lack of collisions invalidates the method. In the two former cases, good agreement was claimed between predictions and experimental results, whereas the CFD model in the third case failed to predict a high-superficial-velocity flow transition.

The aim of this article is to examine the variables that control the solid volume fraction in the axial direction under atmospheric and severe operating conditions as well as gas-solid interactions in the bed expansion zone. A thermodynamic correlation as the User-Define-Function (UDF) was included to evaluate the influence of the gas on the solid particle at high temperature and pressure at 650 K and 1 MPA.

Also, to study the effect of operating conditions such as superficial gas, type of materials, particle size, mesh sensitivity and time dependence of the system in order to evaluate the influence on these parameters. Furthermore, the aimed at creating a more robust geometry to show complexity in the evaluation of the hydrodynamic parameters in 3D, making the study of discretization of the computational domain more noteworthy, and demonstrating the effectiveness of the models selected for this study.

II. COMPUTATIONAL FLUID DYNAMIC MODEL

This section describes the mathematical modeling of the problem addressed in this work, which is the hydrodynamic theory for multiphase flows, implemented in the Ansys@ Fluent programming platform. The fluidized beds were modeled as multiphase flows comprising two-phases, a gas phase and a solid-particles phase. A Euler–Granular approach was employed to model the gas–solid flow. Here, the solid-gas phase is described as interpenetrating fluids (also referred as interpenetrating continua) mapped with respect to a fixed reference frame, as is described in the mapped with respect to a fixed frame of reference (Gibilaro and Felice [13] and Syamlal, Rogers and O’Brien [14]).

A. Dynamical Equations

For the two-phase system described previously, the next continuity equations are considered:

$$\frac{\partial}{\partial t} (\alpha_g \rho_g) + \nabla \cdot (\alpha_g \rho_g \vec{u}_g) = 0, \quad (1)$$

$$\frac{\partial}{\partial t} (\alpha_s \rho_s) + \nabla \cdot (\alpha_s \rho_s \vec{u}_s) = 0. \quad (2)$$

In Eq. (1) and (2), α_i, ρ_i are the volume fraction and mass density of the phase $i = s, g$, respectively; and \vec{u}_g and \vec{u}_s are the velocities of the gas and solid phases, respectively. Additionally, the next momentum balance equations are also considered in the model:

$$\frac{\partial}{\partial t} (\alpha_g \rho_g \vec{u}_g \vec{u}_s) + \nabla \cdot (\alpha_g \rho_g \vec{u}_g \vec{u}_g) = -\alpha_g \nabla P + \nabla \cdot (\bar{\tau}_g + \alpha_g \rho_g \vec{g} - K_{sg} (\vec{u}_s - \vec{u}_g)), \quad (3)$$

$$\frac{\partial}{\partial t} (\alpha_s \rho_s \vec{u}_s \vec{u}_s) + \nabla \cdot (\alpha_s \rho_s \vec{u}_s \vec{u}_s) = -\alpha_s \nabla P + \nabla \cdot (\bar{\tau}_s + \alpha_s \rho_s \vec{g} - K_{sg} (\vec{u}_g - \vec{u}_s)). \quad (4)$$

Here, ∇P , stands for the pressure gradient; $\alpha_i \rho_i \vec{g}$ and $\bar{\tau}_i$, represents the specific gravitational force and tensor stress of the phase $i = g, s$, respectively; and K_{gs} is the gas-solid drag coefficient.

B. Fluid-solid exchange coefficients

The momentum exchange term in Equations (3) and (4) explicitly depends on the gas-solid exchange coefficient K_{sg} , defined for the fluid-solid exchange coefficient—, which has to be adjusted to include the momentum exchange between phases. Therefore, fluid-solid type models have been considered in the present work, proposed by Syamlal and Obrien [14] Gibilaro Visuri and Wierink [15], and the corresponding expressions for K_{st} .

C. Syamlal O'Brien Drag Correlation

Based on the measurement of the terminal velocity of particles in settling beds, the drag model proposed the following drag correlation:

$$f_{gs} = \frac{C_D Re \alpha_l}{24 u_s^2}, \quad (5)$$

$$C_{D,sg} = \left((0.63 + \frac{4.8}{\sqrt{(Re_s/u_s)}}) \right)^2. \quad (6)$$

Where: $C_{D,sg}$ is the solid-gas drag coefficient, Re_s is the solid Reynolds number, α_l is the liquid volume fraction, and u_s is the solid velocity.

D. Gibilaro Drag Correlation

Gibilaro drag function extended its applicability to the gas-particle system by relating the energy dissipation in the fluidized bed with the unrecoverable pressure loss to obtain the particle drag force under the fully expanded limit condition. The Gibilaro drag model is shown below:

$$K_{sg} = \left(\frac{18}{Re_s} + 0.63 \right) \frac{\rho_g \alpha_s (v_s - v_g)}{d_s} \alpha_l^{1.8} \quad (7)$$

The k-epsilon model is available on the CFD software used, Dadashi and Zhang and Alfonsi, G. [16], and platform Guide; they were employed in this research. To evaluate a mesh sensitivity analysis, they were used to determine whether or not mesh dependence exists.

E. Thermodynamic correlation-Peng Robinson-UDF

Cubic equations of state, Smith, J. M., Van Ness, H. C., Abbott, M. M., & García, C. R. [17] are a convenient means for predicting real fluid behavior. In this research, the Peng Robinson correlation Equations (8a-8d) will be used and the behavior of real gas and the influence on gas volume fraction will be analyzed.

$$P = \frac{RT}{v-b} - \frac{a(T)}{v^2 + 2bv - b^2}, \quad (8a)$$

$$b = 0.0778 \frac{RT_c}{P_c}, \quad (8b)$$

$$n = 0.37464 + 1.5422\omega - 0.2699\omega^2, \quad (8c)$$

$$a(T) = 0.45724 \frac{R^2 T_c^2}{P_c} \left[1 + n - n \sqrt{\frac{T}{T_c}} \right]^2. \quad (8d)$$

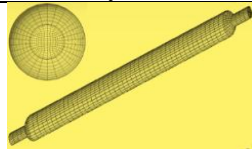
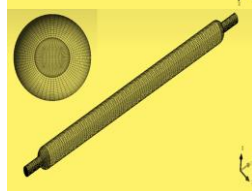
Where ω , is called the acentric factor. In the previous equations, P is the pressure, R is the ideal gas constant, T the temperature, v is the molar volume, and P_c , T_c are the critical pressure and temperature, respectively. The real gas model was implemented into Fluent with User Defined Functions (UDF).

III. SIMULATION SETUP

The laboratory-scale fluidized bed reactor is 0.52 m in diameter and 2.7 m high, and it has a geometry design within the Fluent environment. Two cases of meshing will be explained below and are represented in (see Table I).

The first system was constructed on 3D, the domain was discretized using a uniform hexahedral mesh with 162352 nodes and 156455 cells of the column and the computational domain is schematically displayed in Table 1. The computational geometry used for the simulation consisted of a bottom gas inlet (See Figure 1), a pressure outlet and no-slip at the wall boundary conditions. Transient CFD simulations were carried out with a time step of 10^{-3} s. The first-order upwind scheme was employed for the spatial discretization of the continuity and the momentum and turbulence equations while time was discretized using first-order implicit. The method of finite volume was applied. shows the second system where the mesh was constructed with 17750 nodes and 16380 cell hexahedral mesh. Grid independent testing was conducted in order to ensure varied results and better-enhanced flow understanding. The study was performed in order to evaluate the solid volume fraction and to compare two types of cell sizes employing two turbulence models.

TABLE I. Meshing Generation information.

Mesh	System	Characteristics
Coarse		No. of Nodes: 17750 16380 hexahedral cells Coarse mesh size
Fine		No. of Nodes: 162352 156455 hexahedral cells Fine mesh size

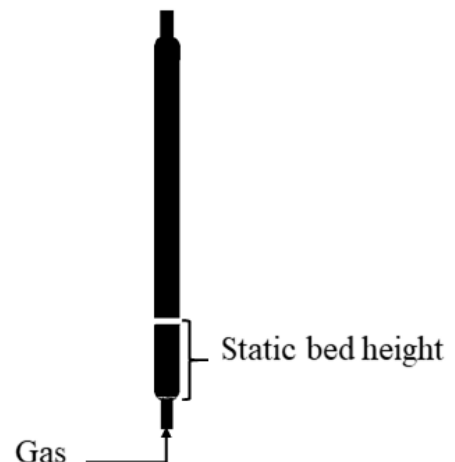


FIGURE 1. The Computational Domain.

IV. RESULTS

The simulation ran a 3D fluidized bed, 2.7 m high, and 0.5 m reactor diameter. The process was carried out at atmospheric conditions. The properties of the materials and the operating conditions that were used in the simulation are presented in Table 2.

3D simulations were performed for 10 s of flow time to allow for complete fluidization. Syamlal O'Brien and Gibilaro drag models were used for the interphases exchange in the fluidization process between such liquid-solid and gas-solid systems.

TABLE II. Simulation and model parameters.

Description	Value	Comment
Drag formulation	Gibilaro Syamlal O'Brien Syamlal O'Brien-drag modification	
Particle density	1654	Kg.m ⁻³
Gas density (air)	1.2	Kg.m ⁻³
Particle diameter	7.5E-5 and 1.6E-2	m
Static bed height H ₀	0.24 and 0.5	m
Initial solid volume fraction ϵ_0	0.5	
Superficial gas velocity1	0.03	m.s ⁻¹
Superficial gas velocity2	0.12	m.s ⁻¹

A. Solid Volume Fraction Interpretation

Axial profiles of solids concentration in previous studies demonstrate that there is a dense phase at the bottom and a dilute phase at the top of the reactor, this is called the *S-shape* profile for bed voidage and with a transition section in between, the reactor may be divided into three regions, a dense region at the bottom portion, a dilute region at the top part and a transition between the two. demonstrated the other profiles, such as S-shape and C-shape, mostly due to the entrance and exit effects as well as the operation conditions.

Y. H. Yu, S. D. Kim [18], Zhu JX. and Cheng Y [19], Li Y. and Kwauk M. [20] and Pärssinen JH. and Zhu J [21]. In the exponential axial profile, the particles are being introduced into the reactor and accelerated upwards very quickly by the fluidization gas to a certain point above the bed catalyst, where the particle velocity becomes constant or to be more precise, the acceleration becomes negligible. A *C-shape* may be observed in a similar system with an abrupt exit. The *S-shape* profile is believed to be related to the high solids flux operation.

Figure 2 represents different inventories of catalysts using the Gibilaro model. It can be seen that the volume fraction of the solid phase reaches almost 35% at the end of the simulation.

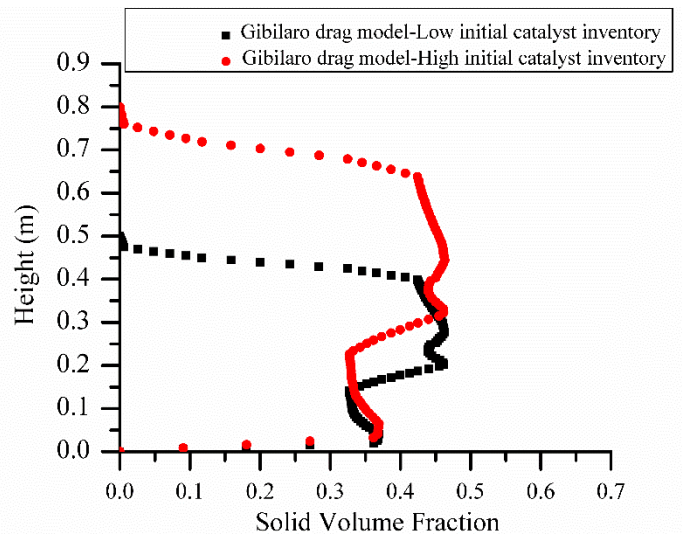


FIGURE 2. The time-averaged solid volume fraction v. the system height with a Gibilaro drag model.

According to the interpretation of solid volume fraction, an *S-shape* is developed in both cases, which means it corresponds to a dense phase located between 0.4 and 0.2 m to the bottom of the reactor. The behavior was very similar, showing that regardless of the initial catalyst inventory established, the solid phase occupied within the catalytic bed shows a very similar trend and, with an increase in the parameter at the same superficial gas velocity, this allows to define that there are changes at the solid volume fraction in relation to the initial bed height, despite the fact that the values of the velocity and particle size remained fixed.

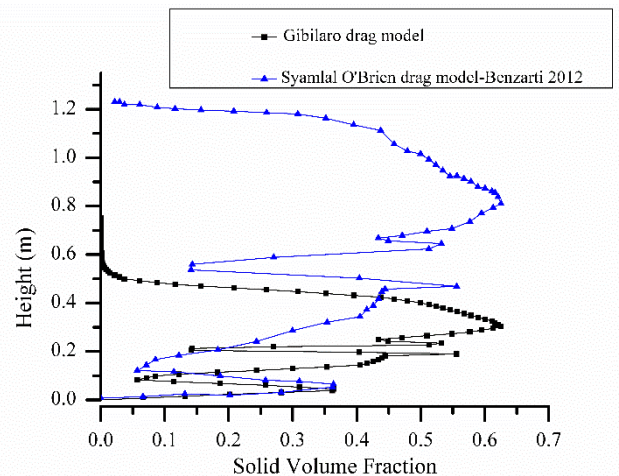


FIGURE 3. The time-averaged solid volume fraction v. the system height with a drag modification function

Figure 3 from the experimental data of Benzarti, S., Mhiri, H., & Bournot, H. [9] a validation was performed using a pure correlation of the Syamlal O'Brien model v. Gibilaro

correlation (to analyze the behavior of the volume fraction of the solid phase under the same operating conditions Benzarti, S., Mhiri, H., & Bournot, H. [9]. It could be observed that the drag model shows that the volume fraction of the solid phase reaches a height of 1.2 m v. a Gibilaro drag model reaches an approximate height of 0.77 m. Nevertheless, the top area of the reactor shows a remarkable *C-shape*. This indicates the formation of a diluted phase, according to interpretation about the solid volume fraction v height. The diluted phase of this formation in the top part of the reactor can be due to the size of the particles used (75 μm). The smaller the particle improves the fluidization process.

Figures 4 and 5 show the distribution of contours of the solid phase during the bed expansion process v. bed height.

The simulations were performed with different superficial gas velocities showing distribution of the solid phase and a high circulation of the gas phase.

The present study also demonstrated that the solid volume fraction increases with respect to the particle density employing the same boundary conditions.

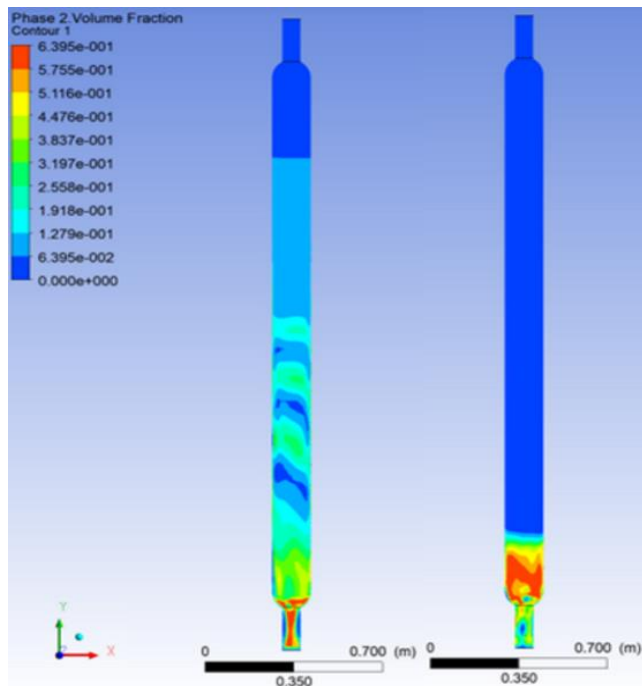


FIGURE 4. Contour plots of the solid volume fraction with Syamlal & O'Brien drag model different superficial gas velocities

Figure 4 shows the contours of the solid volume fraction phase at different gas superficial velocities, 0.03 and 0.12 $\text{m}\cdot\text{s}^{-1}$ using the Gibilaro drag model, despite the inlet velocity; there is a significant displacement of the catalyst bed clustering towards the walls of the reactor in an inclined manner, and the solid phase remains at the bottom of the reactor. On the contrary, the following scheme shows the interaction of the phases in a more distributed and uniform

manner, and a greater solid concentration in the center of the reactor.

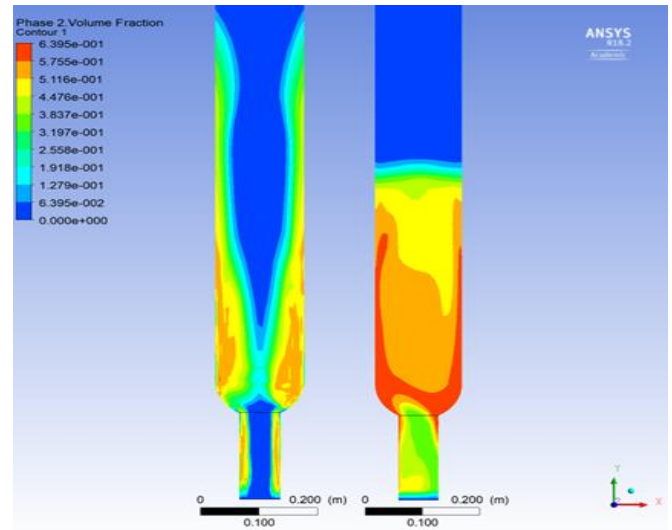


FIGURE 5. Effect of different materials on transient solid volume fraction in the equilibrium state ($u=0.03 \text{ m/s}$).

Figure 5 shows the contour of the solid phase, employing different materials with different types of particle size for the simulations at the same superficial gas velocities. In the scheme on the left-hand side, the solid phase is located near the walls and creates a split in the center of the reactor. In this case, a material with a density of $2,700 \text{ kg}\cdot\text{m}^{-3}$ and particle diameter of $2.18\text{E}-3 \text{ m}$ was used. The scheme on the opposite side illustrates the material presented by Benzarti showing more consistency of the results obtained in their research: a better behavior of the volume fraction of the solid phase v. reactor height. This is associated to (i) the size of the particles and the void initial fraction; (ii) a homogenization between the two phases; (iii) positioning at the height of the bed and not creating an exaggerated expansion, which does not occur in the fluidization process

V. DISCUSSION

A. Mesh Sensitivity Study

Figure 6 and 7 show the comparison between a coarse (right) and a fine (left) mesh, evaluating the volume fraction and the axial velocity of the solid phase, which indicates that using the *k-epsilon* turbulence model, in both cases, simulates reasonably well. The results below indicate that there is a relative mesh dependence for both fine and coarse meshes according to the cells size used to build the grid. Therefore, the values for axial velocities of the solid phase were far from the values expected. This will be explained in detail further down.

Figure 6 depicts the solid volume fraction. Employing Gibilaro's drag model with a fine mesh (right), there is no

expansion beyond the initial height zone of the defined bed. It is also observed that there is a mix of the phases. However, in the case of the coarse mesh (left), an increase can be observed. It highlights how the gas is occupying the top part of the bed and trying to push the solid phase to the center of the reactor.

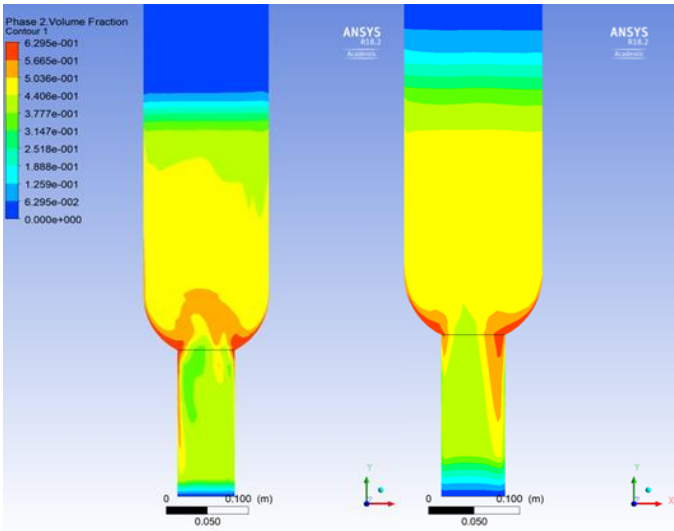


FIGURE 6. Solid volume fraction employing the Fine and Coarse Mes.

moving inside the bed expansion zone and remain stable during the process. Nevertheless, the fine mesh starts with a velocity at $0.09 \text{ m}\cdot\text{s}^{-1}$ and increases to a peak of ($0.20 \text{ m}\cdot\text{s}^{-1}$) at 0.15 m . Velocity decreases up to a height of 0.4 m , and increases again, reaching its maximum ($0.16 \text{ m}\cdot\text{s}^{-1}$) in at the 0.5 m height, where the steady state is reached. These simulations were performed under the same operating conditions, superficial gas velocity, and initial conditions of solid phase.

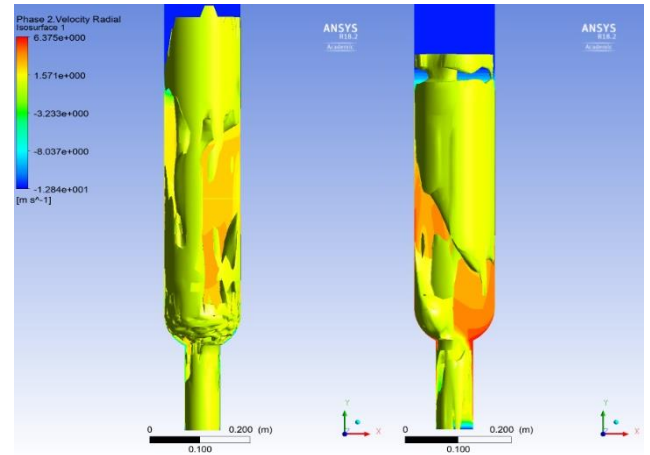


FIGURE 8. Radial profile of solid velocities in a Coarse and Fine Mesh employing k-epsilon Turbulence Model.

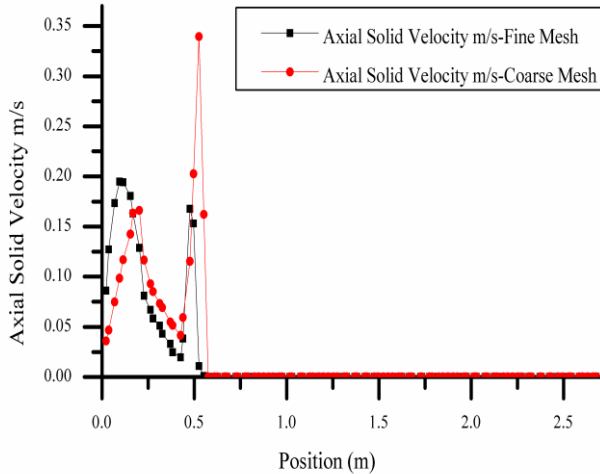


FIGURE 7. Axial profile of vertical solid velocities in a Coarse and Fine Mesh employing k-epsilon Turbulence Model.

Figure 7 exhibits the axial solid velocity as a function of the position of the fluidized bed reactor. The velocity in the coarse mesh was low at the beginning ($0.025 \text{ m}\cdot\text{s}^{-1}$), but increased significantly in 0.25 m reaching ($0.17 \text{ m}\cdot\text{s}^{-1}$).

However, maximum axial solid velocity in the coarse mesh was achieved at a height of 0.5 m with a velocity of ($0.35 \text{ m}\cdot\text{s}^{-1}$). This indicates that an interaction between the gas and solid phase is occurring. Afterward velocity falls to zero in 0.6 meters , denoting that only the particles are

In Figure 8, the radial profile velocity of solid phase is outlined, showing that at a height of approximately 0.5 meters there is a strong concentration of the solid phase (fine mesh to the right, coarse mesh to the right). It demonstrates that the gas and solid phase create an impact during the fluidization process, located in the central part of the domain.

The radial velocity of the solid phase is one of the most interesting parameters to analyze for these types of cases in three dimensions, where it is observed in detail the movements of the particles and their mixture with the gas phase. This indicates that there is represent the contact between them and the behavior is associated with a real fluidization process.

B. Time Dependence Study

Simulations were performed using different time step conditions to examine the changes of solid volume fraction. According to the simulation time variations there is an influence on this hydrodynamic parameter.

Figure 9 the results of the solid phase were compared at a time step of 0.100 s and 0.001 s at times of 30 seconds . The contour on the left shows an agglomeration of particles on the reactor's walls, which could corroborate the theory in relation to the time step size. Furthermore, there is no uniform distribution of the solid phase, as shown in the scheme on the right, where the time step size was small, but, in this case, a bed expansion is observed and, while the

process goes on, the particles look for ways to occupy the region near the walls of the system.

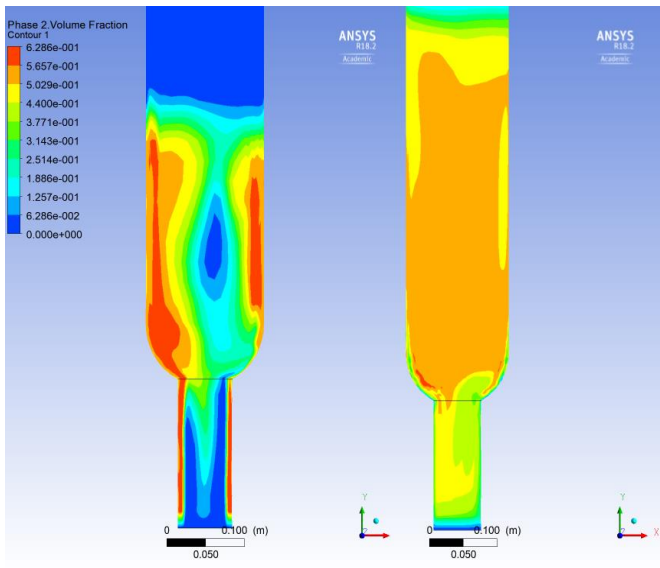


FIGURE 9. Contour plots of the solid volume fraction with different time step (left 0.100 s) (right 0.001 s).

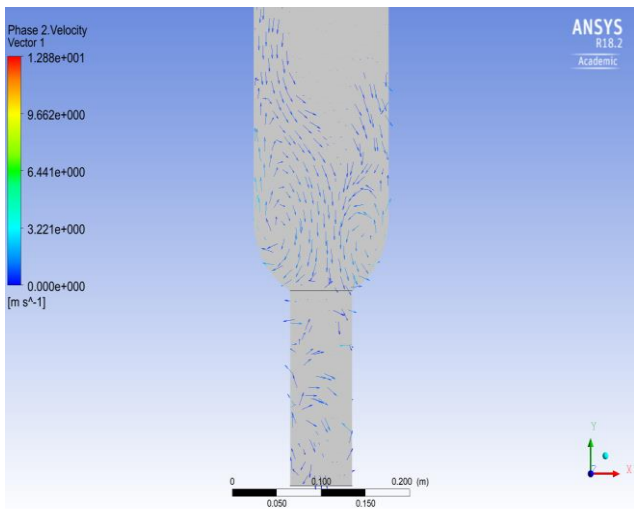


FIGURE 10. Velocity Vector on the $y=0$ Plane.

In Figure 10 the circulation of the solid in the inlet and the fluidization zone are observed, showing swirls and eddies in the lower part of the reactor, representing the mixture of both phases, and how the solid is retained on the walls of the reactor.

Thus, the selection of a suitable time for the solution of the domain is essential to avoid errors in the final results, which would produce no convergence and jumps in the cells that are being analyzed.

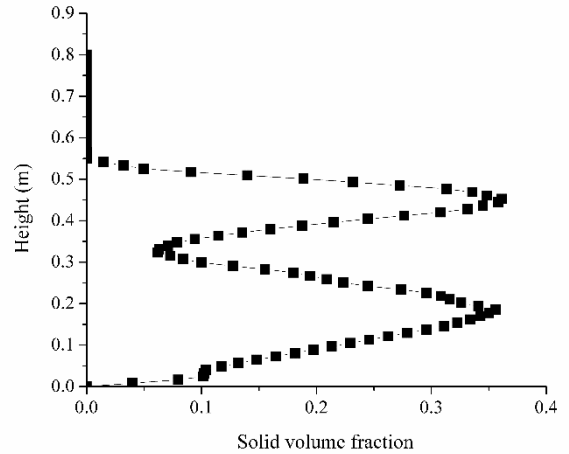


FIGURE 11. Solid volume fraction- time step 0.100 s.

Figure 11 points out the different solid volume fractions obtained by changing the height of the fluidized bed. No dense phase formation was observed at the top of bed at the height of 0.6 m, contrasting with that depicted in Figure 12, that is the formation of a dense region at the bottom of the reactor and, consequently, a significant expansion of the bed is observed.

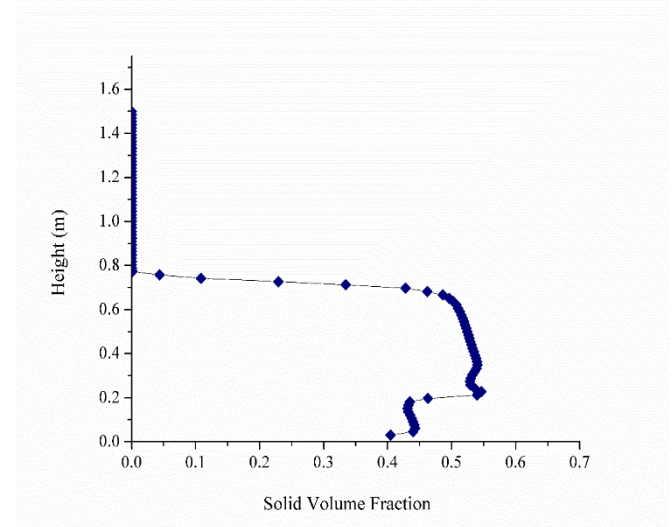


FIGURE 12. Solid volume fraction time step-0.001s

C. Severe condition employing a UDFs

A User Defined Function (UDF) was incorporated into the hydrodynamic model. We selected the Peng-Robinson thermodynamic equation, considering a non-ideal gas, operated at a temperature of 650K and 1 MPa. These conditions were used to determine the behavior of the solid phase at severe conditions of temperature and pressure. The gas-phase (hydrogen) and solid phase (nickel-molybdenum) were included in the simulation and the

particle distribution was evaluated under these conditions, using the Gidaspow drag correlation [22].

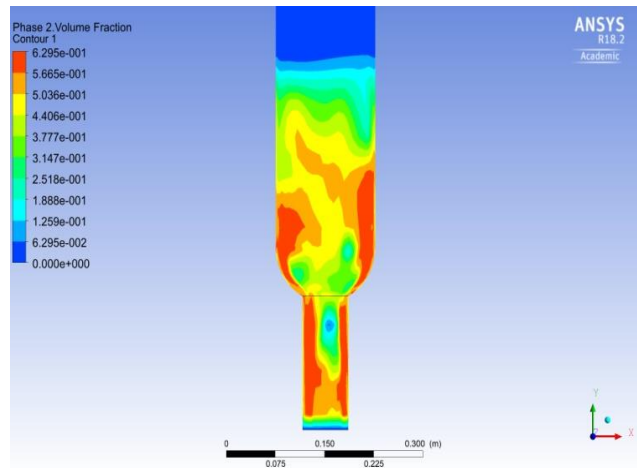


FIGURE 13. Contour plots of the solid volume fraction at severe condition at 1 MPA and 650 K.

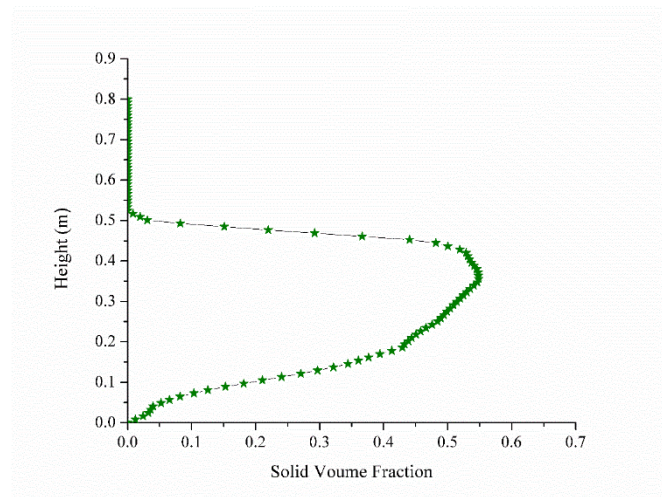


FIGURE 14. Solid volume fraction at severe condition.

In Figures 13 and 14, there is a greater concentration of the solid phase on the walls and in the bottom region of the reactor. Increased bead expansion was found, setting up a dense phase. The thermodynamic correlation and drag model demonstrated the S-shape, greatly influenced by severe conditions of high pressure and temperature.

VI. CONCLUSIONS

The average solid volume fraction in a liquid-solid and gas-solid circulating fluidized bed was examined for three different conditions: superficial gas velocity, catalyst inventory, and different type of particle in order to evaluate the hydrodynamic behavior. The following are the conclusions drawn during the present research:

The solid volume fraction profile can be affected by some operating variables such as superficial gas velocity, bed diameter, particle properties, density, size distribution, total solids inventory, among others. With a higher solids flux, a denser bed can be observed and the transition region between the dense bed and the dilute phase occurs higher up in the reactor. The lower the solids flux, the less solids volume fraction exists in the reactor and it is affected by the superficial gas velocity. During the mesh sensitivity study, it was found that there is a mesh dependence, using the *k*-epsilon turbulence model and it showed a different behavior establishing the same operating conditions and boundaries for all the cases presented. There is a dependence on the time step since variations regarding time step size change significantly the final result of the parameters being evaluated. As a result, it is fundamental to make an appropriate selection of the cell size and to check if there is an association between the selected models. When the gas conditions change from the standard condition to severe conditions of pressure and temperature, the formation of the dense phase at the bottom of the reactor is observed in the solid volume fraction.

ACKNOWLEDGMENTS

This study was supported by the Conacyt Institute in Mexico and The Research Center for Applied Science and Advanced Technology (CICATA).

REFERENCES

- [1] Kallio, S., Peltola, J., & Taivassalo, V., Characteristics of the solid volume fraction fluctuations in a CFB, (2011).
- [2] Kuramoto, K., Tanaka, K., Tsutsumi, A., Yoshida, K., & Chiba, T., *Macroscopic flow structure of solid particles in circulating liquid-solid fluidized bed riser*, Journal of chemical engineering of Japan **31**, 258-265 (1998).
- [3] Liang, W. G., & Zhu, J. X., *Effect of radial flow non uniformity on the alkylation reaction in a liquid- Solid circulating fluidized bed (LSCFB) reactor*, Industrial & Engineering Chemistry Research **36**, 4651-4658 (1997).
- [4] Natarajan, P., Velraj, R., & Seeniraj, R. V., *Hydrodynamic similarity in liquid-solid circulating fluidized bed risers*, Powder Technology **264**, 166-176. (2014).
- [5] Ding, J., & Gidaspow, D., *A bubbling fluidization model using kinetic theory of granular flow*, AIChE Journal **36**, 523-538 (1990).
- [6] Zimmermann, S., & Taghipour, F., *CFD modeling of the hydrodynamics and reaction kinetics of FCC fluidized-bed reactors*, Industrial & Engineering Chemistry Research **44**, 9818-9827 (2005).
- [7] Taghipour, F., Ellis, N., & Wong, C., *Experimental and computational study of gas-solid fluidized bed hydrodynamics*, Chemical Engineering Science **60**, 6857-6867 (2005).

- [8] Johnson P. C., Jackson R., *Frictional-collisional constitutive relations for granular materials, with application to plane shearing*, J. Fluid Mech **176**, 67–93 (1987).
- [9] Benzarti, S., Mhiri, H., & Bournot, H., *Drag models for simulation gas-solid flow in the bubbling fluidized bed of FCC particles*, World Academy of Science, Engineering and Technology **61**, 1138-1143 (2012).
- [10] Gidaspow, D., Bezburuah, R., & Ding, J., *Hydrodynamics of circulating fluidized beds: kinetic theory approach*, Illinois Inst. of Tech., Chicago, IL United States, Dept. of Chemical Engineering (1991).
- [11] Roy, S., & Dudukovic, M. P., *Flow mapping and modeling of liquid– solid risers*, Industrial & engineering chemistry research **40**, 5440-5454 (2001).
- [12] Lettieri, P., Cammarata, L., Micale, G.D.M., Yates, J., *CFD simulation of gas fluidized beds using alternate Eulerian–Eulerian modeling approaches*, International Journal of Chemical Reactor Engineering **1**, (2001).
- [13] Gibilaro, L. G., Di Felice, R., Waldram, S. P., & Foscolo, P. U., *Generalized friction factor and drag coefficient correlations for fluid-particle interactions*, Chemical engineering science **40**, 1817-1823 (1985).
- [14] Syamlal, M., & O'Brien, T. J., *Computer simulation of bubbles in a fluidized bed*, In AIChE Symp. Ser **85**, 22-31, (2001).
- [15] Visuri, O., Wierink, G. A., & Alopæus, V., *Investigation of drag models in CFD modeling and comparison to experiments of liquid–solid fluidized systems*, International Journal of Mineral Processing **104**, 58-70 (2012).
- [16] Dadashi, A., Zhu, J. J., & Zhang, C., *A computational fluid dynamics study on the flow field in a liquid–solid circulating fluidized bed riser*. Powder technology **260**, 52-58 (2014).
- [17] Smith, J. M., Van Ness, H. C., Abbott, M. M., & García, C. R., *Introducción a la termodinámica en ingeniería química*, (McGraw-Hill, México, 1989).
- [18] Yu, Y. H. Kim, S. D., *Bubble characteristics in the radial direction of three-phase fluidized beds*, AIChE Journal **34**, 2069-2072 (1988).
- [19] Zhu, J. X. and Cheng, Y., *Fluidized-Bed Reactors and Applications*, Chapter 5.3 in Multiphase Flow Handbook, ed. Clayton Crowe, (CRC Press, New York, 2005), pp 5.55-5.93.
- [20] Li, Y. and Kwauk, M., *The dynamics of fast fluidization Fluidization*, Grace, J. R. and Matsen, J. M. (Plenum Press, New York, 1980), pp. 537-544.
- [21] Pärssinen J. H. and Zhu J., *Particle velocity and flow development in a long and high flux circulating fluidized bed riser*, Chemical Engineering Science **56**, 5295-5303 (2001).
- [22] Gidaspow D., *Multiphase Flow and Fluidization: Continuum and Kinetic Theory Descriptions*, (Elsevier Science, USA, 1994).